Revision 2

Zircon growth and recrystallization during progressive metamorphism, Barrovian zones, Scotland

Sarah H. Vorhies[1], Jay J. Ague[1, 2], and Axel K. Schmitt[3]

[1]Department of Geology and Geophysics
Yale University
P.O. Box 208109
New Haven, CT 06520-8109

[2]Peabody Museum of Natural History
Yale University
New Haven, CT 06511

[3]Department of Earth and Space Sciences
University of California Los Angeles
595 Charles Young Dr. E
Los Angeles CA 90095

Always consult and cite the final, published document. See http://www.minsocam.org or GeoscienceWorld

ABSTRACT

The effect of progressive metamorphism (Grampian orogeny) and later tectonic activity on detrital zircon in the Barrovian zones of Scotland was studied using secondary ion mass spectrometry (SIMS) and backscattered electron imaging (BSE). Fifteen samples recording progressive metamorphism from the chlorite through the sillimanite−K-feldspar zones were investigated by: (1) SIMS U-Pb depth profiling into rims of unpolished zircon grains to analyze sub-μm−scale features and (2) conventional spot analysis on sectioned and polished grains. Spot analyses of zircon interiors yield pre-metamorphic detrital ages for all metamorphic grades. Most are in the range ca. 600 to ca. 2000 Ma, but some stretch back to the Archean. Younger ages are recorded in zircon rims, but zircon rim alteration at lower metamorphic grades occurs over much shorter length scales (the outer ~80 nm to ~1 μm of the grain) than in the upper amphibolite to granulite facies (rims of 10 to 30 μm). For example, Grampian (~470 Ma) metamorphism from the garnet and kyanite zones affected only the outermost rims (<1 μm) of detrital zircon grains. Thicker, 10 to 30 μm rims that could be dated by conventional spot analysis developed only at high grades in the sillimanite and sillimanite−K-feldspar zones, probably in the presence of partial melt. The mean Grampian zircon age from spot and depth profile analyses is 472 ± 4 Ma (n=19). In addition to Grampian ages, the zircon depth profiles reveal ages related to five main events that postdate the Grampian Orogeny: decompression melting at ca. 450 Ma; subduction and I-type granite intrusion at ca. 420 Ma; granite intrusion at ca. 384 Ma; extension-related volcanism and vein mineralization at ca. 335 Ma, and further rifting and basaltic magmatism at ca. 250 Ma. These events are recorded only in the very narrow rims (<1 μm) of zircons, and are

Always consult and cite the final, published document. See http://www.minsocam.org or GeoscienceWorld

thus undetectable with conventional spot analysis. We conclude that: (1) zircon interiors were able to retain detrital ages up to and including the highest grade of Barrovian metamorphism (sillimanite-K-feldspar zone) and (2) the <1 μm thick zircon rims may preserve a rich history of metamorphic and post-metamorphic events that can be dated using SIMS U-Pb depth profiling techniques.

Keywords: Barrovian, zircon, U-Pb geochronology, metamorphism, Dalradian

INTRODUCTION

The ability to accurately date both peak and post-peak metamorphic and fluid infiltration events is critical to understanding the geologic history of a metamorphic region. Zircon is an excellent U-Pb geochronometer due to its ability to substitute U and Th, but generally not Pb, into its structure when it crystallizes (e.g., Watson et al. 1997). Zircons are ubiquitous and extremely durable, allowing for their use in dating very old geologic material (e.g., Nemchin et al. 2006; Trail et al. 2007) and in studying provenance of zircon-containing sediments (e.g., Cawood et al. 2003; Fedo et al. 2003; Rahl et al. 2003; Nelson and Gehrels 2007; Gehrels 2012). Zircons have been used to date metamorphism in myriad ways. Discordant ages from detrital zircons can be used to date Pb-loss events (e.g., Gastil et al. 1967; Gebauer and Grünenfelder 1976), which was especially useful before the advent of techniques that allow for focused analysis of single domains within a zircon (Davis et al. 2003). Recently, much work has been done to understand the effect of metamorphism on zircons and to use zircons to better understand the evolution of mountain belts (e.g., Vavra et al. 1999; Rubatto et al. 2001; Breeding et al. 2004;

Always consult and cite the final, published document. See http://www.minsocam.org or GeoscienceWorld

Hay and Dempster 2009). Age determination and geochemical analysis of detrital zircons found in metamorphic rocks have been used to constrain the timing and extent of peak metamorphism and fluid infiltration even when preserved as small-scale features at the rim or in zircon interiors (Carson et al. 2002; Mojzsis and Harrison 2002; Breeding et al. 2004).

In spite of these advances, much remains to be learned regarding which metamorphic grades and conditions will result in recrystallized or newly grown zircon, particularly during progressive, Barrovian-style metamorphism. Our focus is on the classic Grampian metamorphic rocks in the Scottish Highlands, including the Barrovian type locality of Glen Clova. These rocks underwent peak metamorphism at 470-465 Ma (Oliver et al. 2000; Baxter et al. 2002). Tectonic activity in the region, including extensive volcanism and hydrothermal vein formation, continued for approximately another 150 m.y. Due to the continued elevated heat flow in the region (Oliver et al. 2008) and the close proximity to the later igneous intrusions (Fig. 1), it is possible that the rocks in this study were affected by this later tectonic activity. We aim, therefore, to investigate the effects of both peak and post-peak metamorphic, magmatic, and tectonic activity on the zircons from the metamorphic rocks of the Scottish Highlands.

Conventional U-Th-Pb isotopic analysis of zircon by Secondary Ion Mass Spectrometry (SIMS) involves focusing the ion beam on interior domains of a sectioned and polished grain mounted in epoxy. Coupled with backscattered electron (BSE) or cathodoluminescence (CL) images of the sectioned zircons, this “spot” method allows for the analysis of specific domains within a zoned zircon as long as the domains are larger than the size of the beam. “Depth profiling” by SIMS, on the other hand, is a method for analysis of much smaller (tens to hundreds of nm-scale) domains at the unsectioned, unpolished rims of zircons and is uniquely suited to detect changes in the isotopic composition of grains with depth (Carson et al. 2002;

Always consult and cite the final, published document. See http://www.minsocam.org or GeoscienceWorld

Mojzsis and Harrison 2002). This method has been used in one area in the Scottish Highlands, as discussed below, by Breeding et al. (2004).

We present SIMS data from both traditionally sectioned and polished zircons and from depth profiling into unpolished zircon rims. The 15 samples reported in this study are from the chlorite through the sillimanite−K-feldspar zones in the Grampian Highlands of Scotland, with locations ranging from the west to the east coasts (Fig. 1). The goals of the study are to: 1) assess the degree of zircon growth/recrystallization that took place during progressive metamorphism across all metamorphic zones; 2) correlate post-peak ages recorded in the zircons to the ages of the abundant igneous rocks in the region (Fig. 1); and 3) relate internal textural information from zircon grains to isotopic and age data from SIMS analysis.

Geologic setting

The samples are pelitic metasediments from the Dalradian Supergroup, which lies between the Highland Boundary Fault (HBF) and the Great Glen Fault (GGF) in Scotland (Fig. 1). Following Vorhies and Ague (2011), the field area was subdivided into Regions I-III, from northeast to southwest. The original sediments were deposited along the edge of the Iapetus Ocean during an extended period of rifting and subsequent basin closure (Cawood et al. 2003; MacDonald and Fettes 2006). Based upon detrital zircon ages combined with paleocurrent data, the sediment source was mostly Laurentian (Grenvillian) with smaller Lewisian input and with possible input from Baltica (Cawood et al. 2003; Breeding et al. 2004; Banks et al. 2007). Deposition began around 800 Ma and continued until the basin closure around 530 Ma (Cawood et al. 2003).

Always consult and cite the final, published document. See http://www.minsocam.org or GeoscienceWorld

Grampian event

The tectonic events associated with the closure of the Iapetus Ocean are responsible for the metamorphism of the rocks in this study. The orogeny resulted in an increase in metamorphic grade from the HBF northward (Fig. 1), providing the basis for Barrow's (1893; 1912) original study of metamorphic index minerals and the later work of Tilley (1925). Around 490 Ma the initial loading of the Dalradian sediments began with the obduction of the Highland Border Ophiolite (Chew et al. 2010). The Grampian Orogeny continued with the collision of Laurentia with the Midland Valley Arc, and possibly other outboard microcontinents (Oliver et al. 2008; Chew et al. 2010). Following the collisional event, there was slab break-off and a resulting slab window (Oliver et al. 2008) and/or lithospheric extension (Viete et al. 2010). The subsequent rising hot asthenosphere partially melted and rose up to form the Newer Gabbros in the northeast (Oliver et al. 2008). The associated increased heat flow also partially melted the lower crust to form the numerous syn-metamorphic granites in the northeast (Regions I and II).

The combination of collisional tectonics with igneous intrusions during the Grampian Orogeny shaped the pressure−temperature−time paths of the metamorphic rocks. Most of what follows is from Vorhies and Ague 2011 and references therein. After the loading and increase in pressure (*P*) across the entire Grampian terrane, the metamorphic histories of different localities in the study area began to diverge. In the western half of the Highlands, what we refer to herein as Region III, peak *P* in the garnet zone was relatively high, 0.9-1.1 GPa, at temperatures (*T*) between 500 and 630 °C. Peak metamorphism in this region was followed by near-isothermal decompression. Around the Barrovian type locality of Glen Clova, in Region II, maximum pressures were also high (~0.8-0.9 GPa). Peak temperatures, however, were attained at lower pressures during exhumation. At ~0.6 GPa, temperatures increased rapidly as the result of a brief

Always consult and cite the final, published document. See http://www.minsocam.org or GeoscienceWorld

thermal pulse or pulses lasting a total of a few hundred thousand years to a few million years (Ague and Baxter 2007; Vorhies and Ague 2011, Viete et al. 2011). Also in Region II, to the north of Glen Clova in Glen Muick, the rocks reached upper amphibolite−granulite facies conditions of 750-800 °C at ~0.9-1.0 GPa. Pressures at peak-*T* in Region I to the northeast are the lowest observed, at ~0.4-0.5 GPa. These rocks as well as the upper amphibolite−granulite facies rocks of Region II were probably affected by the same tectonometamorphic activity that caused the thermal pulses in Glen Clova.

Current geochronological constraints on the metamorphism consist of garnet−whole-rock Sm-Nd dating, ages of nearby syn-metamorphic igneous intrusions (Fig. 1, Table 1), and U-Pb zircon dating of metamorphic rocks. The Grampian Orogeny is thought to have been relatively rapid, lasting around 15 m.y. (Oliver et al. 2000; Dewey 2005), with garnet growth lasting ca. 8 m.y., from ca. 473-465 Ma (Baxter et al. 2002). Garnet growth in the garnet, kyanite, and sillimanite zones occurred penecontemporaneously at 467-464 Ma (Baxter et al. 2002). In order to further constrain the age of metamorphism Breeding et al. (2004) carried out SIMS depth-profiling on zircons from a rock in our Region I. Ague (1997) previously determined that fluid flow through fractures had altered the chemistry and mineral assemblage of a selvage region adjacent to a quartz vein. Zircons from within the vein selvage had a U-Pb lower intercept age of 462 ± 9 Ma with isotopic alteration apparent in the outer 1.3 μm of the zircon grain. The outer ~1 μm of the zircon is marked by an increase in U, Th, and non-radiogenic Pb compared to the more interior portions of the grain. Breeding et al. (2004) concluded that this age reflects zircon growth or recrystallization during the syn-metamorphic fluid infiltration.

The synmetamorphic gabbros are part of a group called the Newer Gabbros which are large, mantle-derived mafic intrusions (Pankhurst 1969; Dempster et al. 2002). The largest of

Always consult and cite the final, published document. See http://www.minsocam.org or GeoscienceWorld

these are the Insch and Morven-Cabrach gabbros, but the group also includes the Haddo House and Portsoy Gabbros. The mafic magmatism was quite extensive at this time, with the thickness of the Insch estimated to be as much as 5,500 m (Clarke and Wadsworth 1970). Many studies have attempted to date different intrusions in the group and most put the age of intrusion at ca. 470 Ma (e.g., Brown et al. 1965; Pankhurst 1970; Dempster et al. 2002). The synmetamorphic granites, such as the Auchlee and Aberdeen, include S-type granites that almost certainly contain a substantial component of partially-melted sedimentary crust (Harmon et al. 1984). Oliver et al. (2008) conclude that the melting was due to increased crustal heat flow caused by a slab window and the associated rising asthenosphere in Regions I and II. The added heat required for the thermal pulses during Grampian metamorphism was likely supplied by these synmetamorphic intrusions (Baxter et al. 2002; Ague and Baxter 2007; Vorhies and Ague 2011). Viete et al. (2011) further postulate that shear heating could also have played a role.

Post-Grampian tectonic events

Following the Grampian event, exhumation continued with little igneous activity until ca. 430 Ma (Fig. 1, Table 1). There is one intrusion dated at 457 Ma (in addition to others in other Scottish terranes) which has been attributed to decompression melting during exhumation of the Grampian crust (Oliver et al. 2008). Around 430 Ma the final Caledonian collision of Avalonia against the Highland terrane began and was followed first by subduction-related granitic rocks (e.g., Dewey 1971), then by unilateral (Atherton and Ghani 2002) or bilateral (Oliver et al. 2008) slab break-off and another period of asthenospheric upwelling. These events resulted in granitic magmatism between the ages of 430 and 400 Ma. Following these events there is one intrusion at

Always consult and cite the final, published document. See http://www.minsocam.org or GeoscienceWorld

396 Ma (Skene) and another at 390 Ma (Glen Tilt) which are possibly related to the distant Acadian Orogeny (Oliver et al. 2008).

Following the Caledonian orogeny there are a few igneous rocks and vein complexes that may also have affected the rocks in this study. First there was extension-related volcanism to the south of Region III between about 335 and 343 Ma (Monaghan and Parrish 2006). Also in Region III are carbonate veins thought to have originally formed 10-30 m.y. after peak Grampian metamorphism, then reactivated and remineralized in the late Carboniferous or early Permian (Parnell et al. 2000; Anderson et al. 2004).

METHODS

Sample preparation

Samples were crushed and separated using standard density and magnetic separation techniques. An aliquot of zircon grains and the AS3 standard (Schmitz et al. 2003) were hand-picked and placed onto double-sided tape, then cast in epoxy. The epoxy mounts were sectioned to reveal grain interiors, polished using ¼ µm diamond paste, cleaned ultrasonically, rinsed with 1 *N* HCl, and coated with ~10 nm of Au using a sputter coater. Imaging of sectioned grains was done using backscattered electron imaging (BSE) on the JEOL JXA-8530F electron microprobe at Yale University. Additional zircons were hand-picked and pressed into indium (In) metal and left unpolished. Standard AS3 crystals were pressed into the mount and polished prior to the addition of the unknown zircons. The In mount was cleaned ultrasonically, rinsed with 1 *N* HCl, and coated with ~10 nm of Au.

Always consult and cite the final, published document. See http://www.minsocam.org or GeoscienceWorld

SIMS analysis

SIMS analysis of zircons was performed at the University of California, Los Angeles on the CAMECA ims 1270 using previously published techniques (Schmitt et al. 2003; Breeding et al. 2004). An $^{16}O^-$ primary beam at 10 keV was focused to a ~15 µm spot diameter. Oxygen flooding was used to increase Pb^+ yields. Secondary ions of $^{94}Zr_2{}^{16}O$ (counting time = 1 s), ^{204}Pb (3 s), ^{206}Pb (6 s), ^{207}Pb (7 s), ^{208}Pb (4 s or 2 s, depending on session), ^{232}Th (2 s), ^{238}U (3 s), $^{238}U^{16}O$ (2 s) were measured in peak jumping mode with individual sweeps over this mass range constituting an analysis cycle. Three techniques were used in this study. First is the conventional analysis of sectioned zircons cast in epoxy. Hereafter called "spot" analyses, these took ~12 minutes each and resulted in a pit ~0.75 µm deep. Two types of depth profiling were also used, wherein the analyses were done into the unpolished rims of whole zircon grains mounted in indium (In). "Short depth profiles" (SDPs) were done under the same conditions as the epoxy spots, resulting in ~15 µm wide and ~0.75 µm deep pits. Pit size and shape was measured using a MicroXAM-100 3D surface profiler and optical interferometer at UCLA. This information was used to estimate sputter rates. Analyses are separated into "blocks" which interpolate intensities between two consecutive magnet cycles. Each block represents ~75 nm of depth. Since the SDPs were done without narrowing the field aperture with depth there is a degree of isotopic mixing that occurs during analysis. The relative contribution of surface-derived ions can be estimated by measuring the Au content at each cycle, as the samples are coated with Au. A depth profile done on standard grain 91500 (Wiedenbeck et al. 2004) shows that the surface Au signal decays approximately exponentially. After 7 cycles the Au signal is ~50% of the original signal and after 9 cycles (the depth of the SDPs done in this study) the Au signal is ~40% of the original. We can use this to algebraically estimate the actual age of the zircons at cycle 9 given the rim

Always consult and cite the final, published document. See http://www.minsocam.org or GeoscienceWorld

age and the apparent age at cycle 9. For example, the $^{206}Pb/^{238}U$ age of cycle 1 from analysis 41A_2_2 (Fig. 7) is 477 Ma and the apparent $^{206}Pb/^{238}U$ age of cycle 9 is 940 Ma. The actual age at cycle 9 will be closer to 1250 Ma, given a 40% contribution from cycle 1 and a 60% contribution from cycle 9. The larger the difference between cycle 1 and cycle 9, the larger the difference there will be between the cycle 9 actual and apparent ages. This is a simple model which assumes equal U concentrations and ignores the additional contributions from cycles 2-8.

Calculating the relative contribution of the surface layer for the interior part of short depth profiles (SDP) using Au does not depend on any assumption of similar ionization or collection efficiencies, only that these remain constant throughout the analysis. This is, to a large extent, justified in that data is only collected after an initial pre-sputter time during which sputter equilibrium is achieved. Also, the SDP duration is sufficiently short so that ionization effects remain largely constant throughout the analysis. In any case, we use this calculation as an illustration of the surface contribution effect, and do not aim to quantify interior ages in this way because of the complexities regarding U and age zonation in individual crystals. To be sure that the ages from SDP analyses represent the true rim age without any older, inner age domains mixing in, cycles from SDPs were graphed and carefully selected so that only the youngest cycles were used to calculate the age.

Finally, a “long depth profile” (LDP) was done, lasting ~90 minutes, with the field aperture set smaller than the secondary beam diameter to exclude secondary ions from the edges of the analysis pit and allow for better depth resolution in a deeper pit. Instrumental bias between conventionally sectioned zircon crystals in epoxy mounts, and unsectioned crystals pressed into In is absent based on excellent agreement between rim and interior analyses for rapidly crystallized volcanic zircon (e.g., Bindeman et al. 2006).

Always consult and cite the final, published document. See http://www.minsocam.org or GeoscienceWorld

Concentrations of U and Th were estimated by comparing known values of U/$^{94}Zr_2{}^{16}O$ and Th/$^{94}Zr_2{}^{16}O$ in the AS3 (Schmitz et al. 2003) and 91500 (Wiedenbeck et al. 2004) standard zircons to the same ratios in the unknowns. Corrections for common Pb were made using ^{204}Pb as a proxy for common Pb content. We used anthropogenic Pb ratios ($^{206}Pb/^{204}Pb = 16.2$ and $^{207}Pb/^{204}Pb = 15.3$) from Sañudo-Wilhelmy and Flegal (1994). Overcorrection of $^{207}Pb^{*}$ can occur by using ^{204}Pb as a proxy for common Pb with unresolved minor interferences (e.g., $^{186}W^{18}O$), resulting in apparent reverse discordance. We have tested this by using ^{208}Pb as an alternative proxy for common Pb which mitigates reverse discordance, but concordia ages remain the same as with the ^{204}Pb correction. However, because the ^{208}Pb correction has higher uncertainties for high $^{208}Pb^{*}$ analyses, and for consistency, we report the ^{204}Pb corrected ages only. Data reduction and calculation of U-Pb ages were done using UCLA software (ZIPS v3.0.4 written by C.D. Coath 2005) and Isoplot v4.11 (Ludwig 2008).

Sample descriptions

The zircons exhibit internal features imaged using BSE that are associated either with a detrital origin or with later growth/recrystallization. The detrital portions of the zircons—either the cores or the entire grain—may contain oscillatory zoning which indicates an igneous origin (e.g., Fig. 2J, L) or be completely homogeneous (e.g., Fig. 2A, B). They are often fractured (e.g., Fig. 2B, C, E, F). They also yield ages that are older than the age of deposition (Cawood et al. 2003). Three main features are possible indicators of metamorphic growth or recrystallization (Hoskin and Black 2000; Putnis 2002; Corfu et al. 2003; Harley et al. 2007; Hay and Dempster 2009). (1) unzoned, nonporous rims ranging from sub-micrometer scale to tens of micrometers in width (e.g., Fig. 2I, K). (2) Rims containing micro-pores which terminate in irregular grain edges

Always consult and cite the final, published document. See http://www.minsocam.org or GeoscienceWorld

(e.g., Fig. 2A). (3) Highly porous altered zones throughout the grain which may or may not follow pre-existing zoning (e.g., Fig. 2C, E, G, H, J). The nonporous rims may be either brighter or darker in BSE than the cores, however the porous portions are always brighter than the rest of the grain. The brighter BSE here is due to the higher levels of U in the domains, whereas the darker domains have lower U.

Chlorite zone. Three samples are from the chlorite zone in Region III; all are dominated by the mineral assemblage Qtz+albitic Pl+Ms+Chl (abbreviations from Kretz 1983). Sample 120C is a metapsammite from an outcrop of metapsammitic and metapelitic rocks. The metapsammitic layers contain networks of quartz veins. Many of the zircon grains have <5 μm porous rim overgrowths, although the interiors of most grains are homogeneous (Fig. 2A). Samples 141A and 141B are from an outcrop containing a 1-2m wide quartz-rich vein which metasomatized the surrounding chlorite-rich phyllite. Sample 141A is from the altered portion of the outcrop and consists of large amounts of albitic plagioclase feldspar and altered inclusions of wall rock. The zircons have rim overgrowths as in sample 120C but with more cracks in their interiors (Fig. 2B). Sample 141B is a chlorite-rich phyllite and is inferred to have been the precursor to the metasomatized 141A. The zircons appear similar to those from 141A.

Biotite zone. Sample 4F is from the biotite zone in Region I. It is a coarse biotite schist containing mostly Qtz+Pl+Bt+Ms+Chl. Biotite porphyroblasts are largest (~2 mm) adjacent to large (5-20 cm) quartz veins which cross-cut pre-existing folds. The zircons are often cracked and have homogeneous to lightly-zoned interiors. They have rare porous interior and rim domains (Fig. 2C).

Garnet zone. In Region III, sample 150B1 is from a massive quartz and feldspar vein surrounded by selvage metapelite. The major silicate mineral assemblage is Qtz+Grt+albitic

Always consult and cite the final, published document. See http://www.minsocam.org or GeoscienceWorld

290 Pl+Ms+Chl. A few of the zircons have distinct rim domains (Fig. 2D) and approximately half
291 have interior porous areas (Fig. 2E). Sample 235A from Region II is a garnetiferous
292 metapsammite with the prograde assemblage Qtz+Grt+Pl+Bt+Ms. The surrounding area contains
293 quartz veins ~15-20 cm thick with a few locally smaller quartz veins. There are some rim
294 domains and little interior porosity in the zircons (Fig. 2F).
295 **Staurolite zone.** The staurolite zone sample, 154J, is from an outcrop in Region I
296 containing extensive veining with the abundance and size of the garnet and the staurolite
297 increasing with proximity to veins (Masters and Ague 2005). The sample itself is from one of
298 these near-vein reaction zones and contains Qtz+Grt+Pl+Bt+Ms+St±Chl. The zircons have
299 occasional rim domains and interior porosity similar to those illustrated in Figures 2E and 2F
300 **Kyanite zone.** Sample 242B is from the Barrovian type locality in Region II. It is a
301 garnetiferous schist layered within a primarily metapsammite outcrop. There is no nearby
302 veining. The mineral assemblage is Qtz+Grt+Pl+Bt+Ms. More than half of the zircon grains in
303 the separate have abundant interior porous domains (Fig. 2G).
304 **Sillimanite zone.** All three sillimanite zone samples are from the Barrovian type locality
305 in Region II. Sample 66A is from a migmatitic, metapelitic gneiss containing
306 Qtz+Grt+Pl+Bt+Ms+Sil+Ky. More than half of the zircons contain interior porous domains and
307 one third have rim domains (Fig. 2H). Sample 263A is a veined, pelitic gneiss with large (0.5
308 cm) garnets and the prograde mineral assemblage Qtz+Grt+Pl+Bt+Ms+Sil. Approximately half
309 of the zircons from 263A have interior porous domains, sometimes along pre-existing zonation.
310 Many zircons have distinct, nonporous rims (Fig. 2I). Sample 41A is from a massive, highly
311 migmatitic psammitic gneiss cut by a 1cm vein containing quartz, plagioclase, and muscovite.
312 The mineral assemblage is Qtz+Grt+Pl+Bt+Ms+Sil+Ky . Almost all of the zircons have porous

Always consult and cite the final, published document. See http://www.minsocam.org or GeoscienceWorld

domains; some of these follow possible original zoning and others cross the grain at seemingly random locations.

Sillimanite−K-feldspar zone. These samples were collected in Glen Muick (Baker and Droop 1983; Baker 1985) and in later sections may be referred to as a group rather than as individual samples. All of the samples contain Qtz+Grt+Kfs+Pl+Bt+Sil. The rocks from this area are the highest-grade in the sequence and the outcrops are migmatitic. Mafic granulites containing clinopyroxene+hornblende+garnet crop out nearby (Baker and Droop 1983; Baker 1985). In our samples cordierite did not form because of the relatively high pressures (~0.9-1 GPa). Sample 284A is a massive, coarse, unveined gneiss with bimodal garnet sizes (<1 mm and ~3 mm diameters). Samples 285A and 286B are gneissose and contain cm-scale quartz veins surrounded by coarse sillimanite. Sample 288B is an unveined, sillimanite-rich gneiss containing layers of quartz and ~4 mm garnets. The zircons from sample 284A all contain either oscillatory or irregular zoning. Approximately one third have porous domains along zones (Fig. 2J). Some also have distinct nonporous rims as in 263A (Fig. 2K). Sample 285A zircons have less porosity and none of the wide rims present in 284A. The zircons from 286B and 288B contain abundant cracks at the rims and through the centers of the grains. Most have oscillatory zonation and there is much less porosity than in the zircons from 284A (Fig. 2L).

Zircon behavior during progressive Barrovian metamorphism

Results of all spot analyses with radiogenic Pb content >90% (n=98) are shown on a concordia diagram in Fig. 3 and listed in Supplementary Data Table 1. Concordia ages from spot (n=63), SDP (n=53), and LDP (n=1) analyses are summarized in Fig. 4. All age results are quoted at 2σ uncertainty.

Always consult and cite the final, published document. See http://www.minsocam.org or GeoscienceWorld

Spot analyses

The age results from spot analyses from all zones range from Grampian to ca. 2800 Ma (Fig. 4A). Importantly, in the chlorite through kyanite zones there are no ages from spot analysis younger than 500 Ma. In the sillimanite and sillimanite−K-feldspar zones, however, there are ages that reflect zircon growth or recrystallization during the Grampian Orogeny. The six measured Grampian rim domains result in a concordia age of 468 ± 7 Ma (mean square of weighted deviates of concordance and equivalence, MSWD=0.9). This is identical, within error, to the age of fluid infiltration in the garnet zone of Region I found by Breeding et al. (2004) and to the age range of garnet growth found by Baxter et al. (2002). Additionally, despite the difference in metamorphic grade and the distance between the upper amphibolite−granulite facies rocks of Glen Muick and the rest of Region II, by separating the ages of the two areas there is no indication that they were metamorphosed at different times. The two spot analyses from the sillimanite zone give a combined age of 476 ± 28 Ma (MSWD=0.28) and the four spot analyses from Glen Muick give a combined age of 467 ± 7 Ma (MSWD=1.2).

We can also correlate the appearance of the spot analysis location to the isotopic results. Two main features are visible in BSE: (1) porous bands that are lighter in BSE intensity than the rest of the grain that are found in all zones (e.g., Fig. 2G, J), and (2) nonporous, lobate, homogeneous domains near the rims of grains that cut across pre-existing zonation that are found in the sillimanite and sillimanite−K-feldspar zones (Fig. 2I, K). The geochronological results of analysis of these two types of domains differ. Spots on porous bands, whether they are on the rim, following pre-existing zones, or cross-cutting the grain, result in discordant or nearly discordant ages. Ages that are nearly completely discordant have very high uncertainty. For example, the analysis spot shown in Fig. 2J has an imprecise concordia U-Pb age of 596 ± 220

Always consult and cite the final, published document. See http://www.minsocam.org or GeoscienceWorld

Ma due to the high discordance. All discordant analyses have $^{206}Pb/^{238}U$ ages that are older than 600 Ma and most are older than 1000 Ma, indicating that age resetting in these porous zones has not occurred during Grampian metamorphism and fluid infiltration. These results are not to be taken as actual ages, but are reported to show the high degree of isotopic discordance in these porous bands. In contrast, all concordant Grampian ages detected using spot analyses were performed on nonporous rim domains up to 30 μm in width from the sillimanite and sillimanite−K-feldspar zones (Fig. 2I, K). The only exception to this is one zircon from Glen Muick which appears to be completely metamorphic (JAB288Brow1_14).It is likely that the same type of alteration is responsible for the two different textures seen in BSE imaging: fluid-mediated dissolution-reprecipitation reactions (e.g., Putnis 2009). Other such zircons are seen in environments where fluid infiltration was important (e.g., Wayne and Sinha 1992; Hacker et al. 1998; Hoskin and Schaltegger 2003; Hay et al. 2009). In this process the original zircon composition is metastable and soluble in the local fluid. Porosity develops, allowing the reaction interface to move further into the grain and the new zircon to reprecipitate. This process has been demonstrated in zircons and other minerals under experimental conditions (e.g., Harlov and Dunkley 2010). The rim areas on the zircons that gave concordant Grampian ages were likely affected by the same process. The rim porosity is either on the nanoscale and thus too small to image, or was destroyed by later recrystallization.

Short depth profiles

Short Depth Profile (SDP) ages obtained from the outermost micrometer of zircon rims span from ca. 250 Ma to ca. 2500 Ma (Fig. 4B, Supplementary Data Table 2). As a group, these results differ greatly from the spot analyses in that most of the SDP ages are younger than 800

Always consult and cite the final, published document. See http://www.minsocam.org or GeoscienceWorld

Ma and more than half are of Grampian age or younger. The mean Grampian age derived from 12 SDP analyses from Regions II and III is 474 ± 6 Ma (MSWD=0.94), which is within error of the previously determined Grampian ages as well as the 468 ± 7 Ma age derived from spot analyses in this study. These SDP results can be separated in order to compare the ages by geographical region. For Region I Breeding et al. (2004) determined that the age of fluid infiltration in the garnet zone was 462 ± 9 Ma. In Region II there are eight analyses with ages corresponding to the peak Grampian event from kyanite zone sample 242B, sillimanite zone samples 41A and 263A, and from sillimanite−K-feldspar zone samples 284A and 286B. These are equivalent at 473 ± 7 Ma (MSWD=0.61). In Region III there are four SDP analyses, all from garnet zone sample 150B1, that are equivalent at 483 ± 25 Ma (MSWD=1.7). While it must be noted that the uncertainty of the combined age in Region III is admittedly high, these results are consistent with the hypothesis that the Grampian Orogeny was penecontemporaneous, within error, in all three regions across the Highlands. Furthermore, as with the spot analyses, we can separate out the upper amphibolite−granulite facies Glen Muick samples from the rest of the samples from Region II to show that these ages too are equivalent within error. The SDPs from the Glen Muick rocks have a combined age of 477 ± 8 (n=3, MSWD=0.58) and the SDPs from the other samples from Region II have a combined age of 467 ± 11 (n=5, MSWD=0.49).

There are 23 SDP results that indicate growth/recrystallization after the Grampian Orogeny. As summarized in Figure 5, these results fall into five distinct ages or groups of ages, four of which can be correlated to known local igneous or tectonic events. First there are six analyses that give a combined age of 450 ± 9 Ma (MSWD=1.3). These are from samples 120C (chlorite zone, Region III), 150B1 (garnet zone, Region III), 242B (kyanite zone, Region II), and 263A (sillimanite zone, Region II). This 450 Ma age is during a time recognized by Oliver et al.

Always consult and cite the final, published document. See http://www.minsocam.org or GeoscienceWorld

(2008) to have been marked by decompression and erosion and numerous S-type granitic intrusions, likely the result of decompression melting. While there is only one known igneous intrusion of approximately this age illustrated in the current work (Kennethmont Granite, Fig. 1, Table 1), there are other intrusions of this age to the north of the study area that are not listed in this paper (Oliver et al. 2008). Next there are seven SDP analyses from samples 41A and 263A (sillimanite zone, Region II) that give a combined age of 421 ± 11 Ma (MSWD=0.8). These two samples are close to each other and also very close to the Lochnagar and Glen Doll granites, which intruded at 420 ± 2 Ma and 419 ± 5 Ma, respectively (Table 1). The heat and/or fluid input from these proximal intrusions likely caused the growth/recrystallization seen in the outermost zircon rims from these samples. Five analyses from sillimanite zone samples 41A and 263A (Region II) and garnet zone sample 150B1 (Region I) give a combined age of 384 ± 13 Ma (MSWD=1.4). This age is within error of the age of the Glen Tilt and Skene granites (Table 1). The zircons in this study were likely affected by the same tectonic activity that produced these granites—possibly the Acadian Orogeny (Oliver et al. 2008).

Following the grouping at ca. 385 Ma there are two more ages seen in the SDP rim analyses. Chlorite zone sample 120C from Region III and sillimanite zone sample 41A from Region II have one analysis each which combine to an age of 339 ± 16 (MSWD=0.43). During this time there was extension-related volcanism in the Midland Valley Terrane to the south of the HBF. In particular, just to the south of sample 120C is the Renfrewshire Hills Block of the Clyde Plateau Lavas which was formed at 335 Ma (Monaghan and Parrish 2006). The volcanic rocks from the extension events to the east may have affected sample 41A as well. Finally there is an SDP age of 252 ± 17 Ma from sample 263A (sillimanite zone, Region II). Following the Carboniferous extension, rifting continued and further volcanism occurred in the Midland Valley

Always consult and cite the final, published document. See http://www.minsocam.org or GeoscienceWorld

Terrane. There was basaltic magmatism to the north and to the south of the study area dated as late as ca. 250 Ma and ca. 264 Ma, respectively (Upton et al. 2004). We conclude that the ca. 250 Ma age in sample 263A is likely related to this continued activity in the region.

Interestingly, the SDP results reveal that only two samples below the sillimanite zone record Grampian ages on the outer ~1 um rims of zircons. Sample 242B is from the kyanite zone and has one Grampian age SDP and sample 150B1 is from the garnet zone and has four Grampian age SDPs. Sample 150B1 is heavily veined and, thus, metamorphic vein-related fluids may have helped mediate Grampian zircon growth and/or recrystallization (e.g., Breeding et al., 2004). Post-Grampian rim domains apparently developed more pervasively in the rocks. It is possible that earlier, Grampian-age domains were destroyed by later growth and/or recrystallization, or that such domains never formed in the first place.

Retrograde metamorphism is common throughout the Highlands; small degrees of retrogression are present in most samples studied herein (e.g., chlorite after garnet, biotite, or staurolite; fine-grained muscovite aggregates after aluminosilicates). The SDP results show that post-peak Grampian activity spanned 100 Ma or more, and was associated with pulses of magmatism and/or tectonism. Thus, retrogression had multiple causes, and multiple events are recorded in zircons from one sample, such as in 41A and 263A as described above. Resolution of these tiny age domains is impossible with conventional SIMS techniques, and instead requires depth profiling.

U-Pb internal systematics do not allow us to distinguish between Pb-loss and new growth/recrystallization for this age range. We therefore use compositional evidence and the consistent behavior of samples (i.e. absence of distinct rim regions in some samples, presence in others) as indications to dismiss Pb-loss. Most of the peak and post-peak ages reported have

Always consult and cite the final, published document. See http://www.minsocam.org or GeoscienceWorld

Th/U < 0.1, used as qualitative evidence of metamorphic growth or recrystallization, as opposed to the older, detrital ages reported which usually have higher Th/U. As described previously, the spot analyses of Grampian age are located on homogeneous, rim regions, which we conclude are areas of metamorphic growth/recrystallization. Figure 3B shows the spot analyses on the concordia diagram from 0-600 Ma. The ellipses cluster around ca. 470 Ma and do not extend into younger ages, indicating that recent Pb-loss is not responsible for the ages. Additionally, the post-peak ages that we have reported are in distinct clusters and are the same age as known tectonic events, whereas Pb-loss would produce more of a continuous range of ages approaching the present.

In this context, it is interesting to note that zircon crystals from the sillimanite−K-feldspar zone rocks of Glen Muick lack post-peak rim ages; however this data set only includes six SDP analyses. A recent study of zircons from the Valle D'Arbedo in the Swiss Alps found that rims which had been recrystallized during an earlier episode of metamorphism were not affected by the later Alpine event because recrystallized zircon was more stable (Vonlanthen et al. 2012). Therefore it is possible that the Grampian recrystallization protected the upper amphibolite−granulite facies zircons of Glen Muick from the later events. However, there are many post-peak ages in zircons from the sillimanite zone, which also have wide Grampian rim domains. Zircon stabilization during high-temperature metamorphic recrystallization therefore appears possible, but additional investigation is required to further corroborate this.

Long depth profile

A long depth profile (~5.5 μm) from sample 286B provides evidence constraining the timing of the upper amphibolite−granulite facies metamorphism and partial melting of the rocks

Always consult and cite the final, published document. See http://www.minsocam.org or GeoscienceWorld

in Glen Muick. Fig. 6 shows the $^{206}Pb/^{238}U$ and $^{207}Pb/^{235}U$ ages as well as the Th/U content of the zircon plotted against depth (see also Supplementary Data Table 3). The isotope data from the outer ~1.15 μm of the zircon gives a concordia age of 475 ± 10 Ma. In the inner ~2.5 μm of the depth profile the Th/U is ~0.01 then begins to rise, peaking at ~0.1 at ~2 μm depth. Th/U then drops again and in the outer ~1.15 μm is ~0.017. Elevated Th/U in zircon (above 0.1) is often taken as a sign of melt-present growth because Th is mobilized in melt, with lower values indicating metamorphic growth (Harley et al. 2007). The ages from ~5.1 μm to ~2 μm (the deepest part of the profile) reveal an old inherited core, likely of metamorphic origin. The spike in Th/U corresponds to the sharp drop in zircon age from the older interior to the outer rim age of 475 ± 10 Ma. The spike almost certainly represents mobilization of Th during partial melting during the Grampian event. The reduced Th/U ratio after the spike indicates either that a high-Th accessory mineral (e.g., monazite) incorporated much of the available Th during the initial melting stage and the zircon grew in the presence of that melt, or that the rim growth occurred in the absence of melt.

The long depth profile shows that the Glen Muick rocks underwent metamorphism and partial melting during the Grampian orogeny, a conclusion that is also supported by the spot and SDP data: By combining spot and SDP results from Glen Muick we get an age of 471 ± 6 Ma (n=7, MSWD=1.13). Comparably, the seven spot and SDP results of the other rocks from Region II, not including the Glen Muick samples, combine to give an age of 468 ± 10 Ma (MSWD=0.43). Finally, combining all Grampian-age spot SDP, and LDP data from all samples results in an age of 472 ± 4 Ma (n=19, MSWD=0.5).

Always consult and cite the final, published document. See http://www.minsocam.org or GeoscienceWorld

Spatial variation in SDP ages

Depth profiles in the Barrovian zones reveal that zircon alteration during a given event certainly does not affect every grain in the sample and, moreover, it can affect different parts of the same grain differently. For example, three SDPs were performed on one grain from sample 41A (Fig. 7). The outermost cycle of analysis 2_1 is concordant at 642 ± 110 Ma and cycles 2 and 3 are discordant, but appear to be approximately the same age. Cycles 1 and 2 of analysis 2_2 are concordant at 462 ± 31 Ma. Cycle 1 of analysis 2_3 is discordant with a $^{206}Pb/^{238}U$ age of 713 ± 56 Ma. For all three analyses the innermost cycles (approximately 700 nm depth) are discordant. The gentle slope of results from the youngest to the oldest ages should not be taken as actual ages and represent isotopic mixing during analysis. There may be step functions along the depth profile that have been smoothed out due to age mixing (see discussion in Methods, above).

On the other hand, in some cases multiple depth profiles from the same grain such as those from 263A have the same ages (Fig. 7). All of the cycles from both analysis 1_1 and 1_2 are statistically identical and concordant at 414 ± 24 Ma and 425 ± 27 Ma, respectively. Furthermore, the two analyses together have a concordia age of 419 ± 18 Ma. Since the analysis stops at ~750 nm there is no way to know how deep into the grain this age domain penetrates; however, given the lack of any spot analysis this young it is likely not deeper than a few micrometers.

The variation in extent or depth of alteration across zircon grains likely reflects the locations of pre-existing surface features that allowed for fluid infiltration and nanometer-scale recrystallization (Breeding et al. 2004). The isotopic variation between grains in the same sample can probably be attributed to the location of the zircon in the rock. In this study, as we have not

Always consult and cite the final, published document. See http://www.minsocam.org or GeoscienceWorld

performed analyses *in situ*, we cannot tell if a zircon was located on a grain boundary or enclosed within a larger mineral. Whether or not a zircon is affected by thermal or fluid infiltration events likely depends on whether the heat or fluid has access to the zircon during the event.

CONCLUDING REMARKS

Documentation and interpretation of zircon growth and recrystallization during Barrovian metamorphism is Scotland have been obtained using three different methods: conventional spot analysis of polished grains, short depth profiles (SDP) and a long depth profile (LDP). Conventional spot analyses of sectioned and polished grains demonstrates that zircon interiors retain inherited detrital ages from the Barrovian chlorite zone through the highest grades recorded in the sillimanite-K-feldspar zone. These ages are mostly between ca. 600 Ma and ca. 2000 Ma, but Archean examples were also found. Metamorphism from chlorite to kyanite zone affected only the outer tens to hundreds of nm of zircon rims, if they were affected at all. Rims large enough for spot analysis—at least 20 μm wide—only formed at and above the sillimanite zone.

In order to investigate the ages of smaller rim domains a different approach is necessary. The results of short depth profile (SDP) analysis in this study show that zircons commonly grow or recrystallize during metamorphism at lower grades, however the scale of the age domains is very small (the smallest resolution in this study is ~75 nm). Some SDPs in zircons from the garnet through the sillimanite−K-feldspar zones revealed Grampian ages; however younger ages indicating post-peak growth/recrystallization as young as the Permian were also found. Importantly, the SDPs show that age domains on zircon rims are discontinuous even on the tens of nanometers scale.

Always consult and cite the final, published document. See http://www.minsocam.org or GeoscienceWorld

Fig. 8 shows a summary cartoon of relevant zircon textures discussed in this paper. Interior porous domains that may or may not follow pre-existing zonation are seen at all metamorphic grades. In the sillimanite and sillimanite−K-feldspar zones, wide rim domains can be found that record the age of the peak metamorphism. The porous domains and wide rims probably formed by coupled dissolution-reprecipitation. In all metamorphic zones thin, discontinuous rim domains may be present that allow for age determinations by depth profiling but are too thin for spot analysis. These rims may preserve the ages of peak or post-peak activity.

Finally, whereas SDPs lead to some degree of isotopic mixing, long depth profiles (LDPs) can be used to resolve different ages with increasing depth. One grain in particular illustrates the utility of LDP analyses. By graphing the Th/U content along with the age, we are able to constrain the age of partial melting in the rocks from Glen Muick in the northern portion of Region II and conclude that the upper amphibolite−granulite facies metamorphism occurred during the Grampian Orogeny.

Results show growth/recrystallization during the Grampian event and during post-peak tectonic or magmatic events (Fig. 5). To summarize, the combined Grampian ages are:

- Grampian spot and SDP analyses from Region II, not including the Glen Muick samples (n=7): 468 ± 10 Ma
- Grampian spot and SDP analyses from Glen Muick (n=8): 472 ± 5 Ma
- Grampian SDP analyses from Region III: (n=4): 483 ± 25 Ma
- All Grampian spot, SDP, and LDP analyses (n=19): 472 ± 4 Ma

The post-peak ages and their likely causes are:

- ca. 450 Ma: Post-orogenic decompression melting, intrusion of S-type granites

Always consult and cite the final, published document. See http://www.minsocam.org or GeoscienceWorld

- ca. 417 Ma: Subduction and intrusion of I-type granites such as the Lochnagar granite and Glen Doll diorite
- ca. 384 Ma: Possible effect of the Acadian Orogeny and intrusion of the Glen Tilt and Skene Granites
- ca. 335 Ma: Extension-related volcanism and vein remineralization; formation of the Clyde Plateau Basalts
- ca. 252 Ma: Rifting and basaltic magmatism

Most geochronological studies of Barrovian metamorphism have focused on the northeastern part of the sequence (Regions I and II herein). Our results are consistent with the interpretation that the entire Barrovian sequence, including the sillimanite-K-feldspar rocks of Glen Muick, underwent prograde metamorphism penecontemporaneously, further illustrating that the Grampian orogeny was geologically rapid (Oliver et al. 2000; Baxter et al. 2002; Dewey 2005). Determining how the rates of critical geologic processes, including burial, exhumation, and thermal pulse activity, contributed to this rapid orogenesis poses an exciting set of challenges for future tectono-metamorphic studies.

Acknowledgements

We gratefully acknowledge J. O. Eckert, Jr. for help with the electron microprobe; M. Andrews, C. Bucholz, I. Derrey and J. Stevenson for assistance in the field; and C. McFarlane and an anonymous reviewer for their thoughtful reviews; and the National Science Foundation Directorate for Geosciences (NSF EAR-0509934 and 0744154 to J.J.A.) and The

Always consult and cite the final, published document. See http://www.minsocam.org or GeoscienceWorld

Geological Society of America (Graduate Student Research Grant to S.H.V.) for support. The ion microprobe facility at UCLA is partly supported by a grant from the Instrumentation and Facilities Program, Division of Earth Sciences, National Science Foundation.

Always consult and cite the final, published document. See http://www.minsocam.org or GeoscienceWorld

REFERENCES

Ague, J. J. (1997) Crustal mass transfer and index mineral growth in Barrow's garnet zone, northeast Scotland. Geology, 25, 73-76.

Ague, J. J. and Baxter, E. F. (2007) Brief thermal pulses during mountain building recorded by Sr diffusion in apatite and multicomponent diffusion in garnet. Earth and Planetary Science Letters, 261, 500-516.

Anderson, R., Graham, C. M., Boyce, A. J., and Fallick, A. E. (2004) Metamorphic and basin fluids in quartz–carbonate–sulphide veins in the SW Scottish Highlands: a stable isotope and fluid inclusion study. Geofluids, 4, 169-185.

Atherton, M. P. (1977) The Metamorphism of the Dalradian rocks of Scotland. Scottish Journal of Geology, 13, 331-370.

Atherton, M. P. and Ghani, A. A. (2002) Slab breakoff: a model for Caledonian, Late Granite syn-collisional magmatism in the orthotectonic (metamorphic) zone of Scotland and Donegal, Ireland. Lithos, 62, 65-85.

Baker, A. J. and Droop, G. T. R. (1983) Grampian metamorphic conditions deduced from mafic granulites and sillimanite-K-feldspar gneisses in the Dalradian of Glen Muick, Scotland. Journal of the Geological Society, 140, 489-497.

Baker, A. J. (1985) Pressures and temperatures of metamorphism in the eastern Dalradian. Journal of the Geological Society, 142, 137-148.

Always consult and cite the final, published document. See http://www.minsocam.org or GeoscienceWorld

Banks, C. J., Smith, M., Winchester, J. A., Horstwood, M. S. A., Noble, S. R., and Ottley, C. J. (2007) Provenance of intra-Rodinian basin-fills: The lower Dalradian Supergroup, Scotland. Precambrian Research, 153, 46-64.

Barrow, G. (1893) On an Intrusion of Muscovite-biotite Gneiss in the South-eastern Highlands of Scotland, and its accompanying Metamorphism. Quarterly Journal of the Geological Society, 49, 330-358.

Barrow, G. (1912) On the geology of lower dee-side and the southern highland border. Proceedings of the Geologists' Association, 23, 274-290.

Baxter, E. F., Ague, J. J., and Depaolo, D. J. (2002) Prograde temperature–time evolution in the Barrovian type–locality constrained by Sm/Nd garnet ages from Glen Clova, Scotland. Journal of the Geological Society, 159, 71-82.

Bindeman, I., Schmitt, A., and Valley, J. (2006) U–Pb zircon geochronology of silicic tuffs from the Timber Mountain/Oasis Valley caldera complex, Nevada: rapid generation of large volume magmas by shallow-level remelting. Contributions to Mineralogy and Petrology, 152, 649-665.

Breeding, C. M., Ague, J. J., Grove, M., and Rupke, A. L. (2004) Isotopic and chemical alteration of zircon by metamorphic fluids: U-Pb age depth-profiling of zircon crystals from Barrow's garnet zone, northeast Scotland. American Mineralogist, 89, 1067-1077.

Brown, P. E., Miller, J. A., Grasty, R. L., and Fraser, W. E. (1965) Potassium-Argon Ages of some Aberdeenshire Granites and Gabbros. Nature, 207, 1287-1288.

Always consult and cite the final, published document. See http://www.minsocam.org or GeoscienceWorld

Carson, C. J., Ague, J. J., Grove, M., Coath, C. D., and Harrison, T. M. (2002) U-Pb isotopic behaviour of zircon during upper-amphibolite facies fluid infiltration in the Napier Complex, east Antarctica. Earth and Planetary Science Letters, 199, 287-310.

Cawood, P. A., Nemchin, A. A., Smith, M., and Loewy, S. (2003) Source of the Dalradian Supergroup constrained by U–Pb dating of detrital zircon and implications for the East Laurentian margin. Journal of the Geological Society, 160, 231-246.

Chew, D. M., Daly, J. S., Magna, T., Page, L. M., Kirkland, C. L., Whitehouse, M. J., and Lam, R. (2010) Timing of ophiolite obduction in the Grampian orogen. Geological Society of America Bulletin, 122, 1787-1799.

Clarke, P. D. and Wadsworth, W. J. (1970) The Insch layered intrusion. Scottish Journal of Geology, 6, 7-25.

Corfu, F., Hanchar, J. M., Hoskin, P. W. O., and Kinny, P. (2003) Atlas of Zircon Textures. Reviews in Mineralogy and Geochemistry, 53, 469-500.

Davis, D. W., Krogh, T. E., and Williams, I. S. (2003) Historical Development of Zircon Geochronology. Reviews in Mineralogy and Geochemistry, 53, 145-181.

Dempster, T. J., Rogers, G., Tanner, P. W. G., Bluck, B. J., Muir, R. J., Redwood, S. D., Ireland, T. R., and Paterson, B. A. (2002) Timing of deposition, orogenesis and glaciation within the Dalradian rocks of Scotland: constraints from U-Pb zircon ages. Journal of the Geological Society, 159, 83-94.

Always consult and cite the final, published document. See http://www.minsocam.org or GeoscienceWorld

Dewey, J. F. (1971) A model for the Lower Palaeozoic evolution of the southern margin of the early Caledonides of Scotland and Ireland. Scottish Journal of Geology, 7, 219-240.

Dewey, J. F. (2005) Orogeny can be very short. Proceedings of the National Academy of Sciences of the United States of America, 102, 15286-15293.

Fedo, C. M., Sircombe, K. N., and Rainbird, R. H. (2003) Detrital Zircon Analysis of the Sedimentary Record. Reviews in Mineralogy and Geochemistry, 53, 277-303.

Gastil, G. R., DeLisle, M., and Morgan, J. R. (1967) Some Effects of Progressive Metamorphism on Zircons. Geological Society of America Bulletin, 78, 879-906.

Gebauer, D. and Grünenfelder, M. (1976) U-Pb zircon and Rb-Sr whole-rock dating of low-grade metasediments example: Montagne Noire (Southern France). Contributions to Mineralogy and Petrology, 59, 13-32.

Gehrels, G. (2012) Detrital Zircon U-Pb Geochronology: Current Methods and New Opportunities. In C. Busby and A. Azor, (Eds.), Tectonics of Sedimentary Basins, p. 45-62. John Wiley & Sons, Ltd, Chichester, UK.

Hacker, B. R., Ratschbacher, L., Webb, L., Ireland, T., Walker, D., and Shuwen, D. (1998) U/Pb zircon ages constrain the architecture of the ultrahigh-pressure Qinling-Dabie Orogen, China. Earth and Planetary Science Letters, 161, 215-230.

Harley, S. L., Kelly, N. M., and Moller, A. (2007) Zircon Behaviour and the Thermal Histories of Mountain Chains. ELEMENTS, 3, 25-30.

Always consult and cite the final, published document. See http://www.minsocam.org or GeoscienceWorld

Harlov, D. E. and Dunkley, D. (2010) Experimental high-grade alteration of zircon using alkali- and Ca-bearing solutions: resetting the zircon geochronometer during metasomatism. Abstract V41D-2301 presented at 2010 Fall Meeting, AGU, San Francisco, Calif, 13-17 Dec.

Harmon, R. S., Halliday, A. N., Clayburn, J. A. P., and Stephens, W. E. (1984) Chemical and Isotopic Systematics of the Caledonian Intrusions of Scotland and Northern England: A Guide to Magma Source Region and Magma-Crust Interaction. Philosophical Transactions of the Royal Society of London Series A, Mathematical and Physical Sciences, 310, 709-742.

Hay, D., Dempster, T., Lee, M., and Brown, D. (2009) Anatomy of a low temperature zircon outgrowth. Contributions to Mineralogy and Petrology, 159, 81-92.

Hay, D. C. and Dempster, T. J. (2009) Zircon Behaviour during Low-temperature Metamorphism. Journal of Petrology, 50, 571-589.

Hoskin, P. W. O. and Black, L. P. (2000) Metamorphic zircon formation by solid-state recrystallization of protolith igneous zircon. Journal of Metamorphic Geology, 18, 423-439.

Hoskin, P. W. O. and Schaltegger, U. (2003) The Composition of Zircon and Igneous and Metamorphic Petrogenesis. Reviews in Mineralogy and Geochemistry, 53, 27-62.

Kretz, R. (1983) Symbols for rock-forming minerals. American Mineralogist, 68, 277-279.

Always consult and cite the final, published document. See http://www.minsocam.org or GeoscienceWorld

Ludwig, K. R. (2008) User's Manual for Isoplot 3.70, a Geochronological Toolkit for Microsoft Excel. Berkeley Geochronological Center, Special Publicaiton No. 4, 1-76.

MacDonald, R. and Fettes, D. J. (2006) The tectonomagmatic evolution of Scotland. Transactions: Earth Sciences, 97, 213-295.

Masters, R. and Ague, J. (2005) Regional-scale fluid flow and element mobility in Barrow’s metamorphic zones, Stonehaven, Scotland. Contributions to Mineralogy and Petrology, 150, 1-18.

Mojzsis, S. J. and Harrison, T. M. (2002) Establishment of a 3.83-Ga magmatic age for the Akilia tonalite (southern West Greenland). Earth and Planetary Science Letters, 202, 563-576.

Monaghan, A. A. and Parrish, R. R. (2006) Geochronology of Carboniferous-Permian magmatism in the Midland Valley of Scotland: implications for regional tectonomagmatic evolution and the numerical time scale. Journal of the Geological Society, 163, 15-28.

Nelson, J. and Gehrels, G. (2007) Detrital zircon geochronology and provenance of the southeastern YukonTanana terrane. Canadian Journal of Earth Sciences, 44, 297-316.

Nemchin, A. A., Pidgeon, R. T., and Whitehouse, M. J. (2006) Re-evaluation of the origin and evolution of >4.2 Ga zircons from the Jack Hills metasedimentary rocks. Earth and Planetary Science Letters, 244, 218-233.

Always consult and cite the final, published document. See http://www.minsocam.org or GeoscienceWorld

Oliver, G. J. H., Chen, F., Buchwaldt, R., and Hegner, E. (2000) Fast tectonometamorphism and exhumation in the type area of the Barrovian and Buchan zones. Geology, 28, 459-462.

Oliver, G. J. H., Wilde, S. A., and Wan, Y. (2008) Geochronology and geodynamics of Scottish granitoids from the late Neoproterozoic break-up of Rodinia to Palaeozoic collision. Journal of the Geological Society, 165, 661-674.

Pankhurst, R. J. (1969) Strontium Isotope Studies related to Petrogenesis in the Caledonian Basic Igneous Province of NE. Scotland. Journal of Petrology, 10, 115-143.

Pankhurst, R. J. (1970) The geochronology of the basic igneous complexes. Scottish Journal of Geology, 6, 83-107.

Parnell, J., Baron, M., Davidson, M., Elmore, D., and Engel, M. (2000) Dolomitic breccia veins as evidence for extension and fluid flow in the Dalradian of Argyll. Geological Magazine, 137, 447-462.

Putnis, A. (2002) Mineral replacement reactions: from macroscopic observations to microscopic mechanisms. Mineralogical Magazine, 66, 689-708.

Putnis, A. (2009) Mineral Replacement Reactions. Reviews in Mineralogy and Geochemistry, 70, 87-124.

Rahl, J. M., Reiners, P. W., Campbell, I. H., Nicolescu, S., and Allen, C. M. (2003) Combined single-grain (U-Th)/He and U/Pb dating of detrital zircons from the Navajo Sandstone, Utah. Geology, 31, 761-764.

Always consult and cite the final, published document. See http://www.minsocam.org or GeoscienceWorld

Rubatto, D., Williams, I. S., and Buick, I. S. (2001) Zircon and monazite response to prograde metamorphism in the Reynolds Range, central Australia. Contributions to Mineralogy and Petrology, 140, 458-468.

Sañudo-Wilhelmy, S. A. and Flegal, A. R. (1994) Temporal variations in lead concentrations and isotopic composition in the Southern California Bight. Geochimica et Cosmochimica Acta, 58, 3315-3320.

Schmitt, A. K., Grove, M., Harrison, T. M., Lovera, O., Hulen, J., and Walters, M. (2003) The Geysers - Cobb Mountain Magma System, California (Part 1): U-Pb zircon ages of volcanic rocks, conditions of zircon crystallization and magma residence times. Geochimica et Cosmochimica Acta, 67, 3423-3442.

Schmitz, M. D., Bowring, S. A., and Ireland, T. R. (2003) Evaluation of Duluth Complex anorthositic series (AS3) zircon as a U-Pb geochronological standard: new high-precision isotope dilution thermal ionization mass spectrometry results. Geochimica et Cosmochimica Acta, 67, 3665-3672.

Tilley, C. E. (1925) A Preliminary Survey of Metamorphic Zones in the Southern Highlands of Scotland. Quarterly Journal of the Geological Society, 81, 100-112.

Trail, D., Mojzsis, S. J., and Harrison, T. M. (2007) Thermal events documented in Hadean zircons by ion microprobe depth profiles. Geochimica et Cosmochimica Acta, 71, 4044-4065.

Always consult and cite the final, published document. See http://www.minsocam.org or GeoscienceWorld

Upton, B. G. J., Stephenson, D., Smedley, P. M., Wallis, S. M., and Fitton, J. G. (2004) Carboniferous and Permian magmatism in Scotland. Geological Society, London, Special Publications, 223, 195-218.

Vavra, G., Schmid, R., and Gebauer, D. (1999) Internal morphology, habit and U-Th-Pb microanalysis of amphibolite-to-granulite facies zircons: geochronology of the Ivrea Zone (Southern Alps). Contributions to Mineralogy and Petrology, 134, 380-404.

Viete, D. R., Hermann, J., Lister, G. S., and Stenhouse, I. R. (2011) The nature and origin of the Barrovian metamorphism, Scotland: diffusion length scales in garnet and inferred thermal time scales. Journal of the Geological Society, 168, 115-132.

Vonlanthen, P., Fitz Gerald, J. D., Rubatto, D., and Hermann, J. r. (2012) Recrystallization rims in zircon (Valle d'Arbedo, Switzerland): An integrated cathodoluminescence, LA-ICP-MS, SHRIMP, and TEM study. American Mineralogist, 97, 369-377.

Vorhies, S. H. and Ague, J. J. (2011) Pressure-temperature evolution and thermal regimes in the Barrovian zones, Scotland. Journal of the Geological Society, 168, 1147-1166.

Watson, E. B., Chemiak, D. J., Hanchar, J. M., Harrison, T. M., and Wark, D. A. (1997) The incorporation of Pb into zircon. Chemical Geology, 141, 19-31.

Wayne, D. M. and Sinha, A. K. (1992) Stability of Zircon U-Pb Systematics in a Greenschist-Grade Mylonite: An Example from the Rockfish Valley Fault Zone, Central Virginia, USA. The Journal of Geology, 100, 593-603.

Always consult and cite the final, published document. See http://www.minsocam.org or GeoscienceWorld

Wiedenbeck, M., Hanchar, J. M., Peck, W. H., Sylvester, P., Valley, J., Whitehouse, M., Kronz, A., Morishita, Y., Nasdala, L., Fiebig, J., Franchi, I., Girard, J. P., Greenwood, R. C., Hinton, R., Kita, N., Mason, P. R. D., Norman, M., Ogasawara, M., Piccoli, P. M., Rhede, D., Satoh, H., Schulz-Dobrick, B., Skår, O., Spicuzza, M. J., Terada, K., Tindle, A., Togashi, S., Vennemann, T., Xie, Q., and Zheng, Y. F. (2004) Further Characterisation of the 91500 Zircon Crystal. Geostandards and Geoanalytical Research, 28, 9-39.

Always consult and cite the final, published document. See http://www.minsocam.org or GeoscienceWorld

FIGURE CAPTIONS

TABLE 1. Ages of relevant igneous rocks within the study area including abbreviations found in Fig. 1.

FIGURE 1. A. Map of the Scottish Highlands indicating metamorphic zones, locations of igneous rocks, and western sample locations. The three major regions are I: along the eastern coast, II: Glen Clova and surrounding glens, and III: the western half of the Highlands. B. Detail of northeastern portion of study area showing sample locations from Regions I and II. All samples include the prefix JAB, which has been omitted throughout the text. Key to abbreviations and more information on each formation is given in Table 1. Modified from Atherton (1977); Ague and Baxter (2007); BGS (2007); and Vorhies and Ague (2011).

FIGURE 2. BSE images of zircons from this study showing A. smooth, homogeneous core with minor porous overgrowth, B. cracked grain, C. occasional porous grain interior, D. thin rim domain, E. minor interior porosity, F. thin rim domain, G. interior porosity that does not appear to follow pre-existing zonation, H. interior porosity, thin rim domain, I. nonporous Grampian age rim domain wide enough for ion beam spot, J. porosity that follows zoning which resulted in a highly uncertain, nearly discordant age, K. nonporous Grampian rim domain, and L. pre-existing oscillatory zoning. Black ovals indicate analysis spots, where appropriate.

FIGURE 3. A. Concordia diagram showing all polished-grain spot analyses with radiogenic Pb > 90%. Error ellipses are plotted at 1σ. Concordia ages indicated in Ma. Box

Always consult and cite the final, published document. See http://www.minsocam.org or GeoscienceWorld

indicates extent of part B of this figure. B. An enlargement of the box on concordia diagram in A, focused on the area from 0-600 Ma.

FIGURE 4. A. Ages of spot analyses plotted against metamorphic zone. Grey line indicates approximate age of the Grampian Event. B. Ages of short depth profile (SDP) and long depth profile (LDP) analyses plotted against metamorphic zone. Grey line indicates approximate age of the Grampian Event.

FIGURE 5. Schematic of SDP and spot results. Grampian results illustrate the synchroneity of orogenic activity across the study area. Zircon ages from this study indicate that the rocks have been affected by four post-peak tectonic events. Error bars and width of grey bar indicate 2σ uncertainty.

FIGURE 6. Long depth profile (LDP) from sillimanite−K-feldspar zone sample 286B (Glen Muick). $^{206}Pb/^{238}U$ and $^{207}Pb/^{235}U$ ages and Th/U content plotted against profile depth into grain.

FIGURE 7. Examples of depth profiles showing the differences in results from three analyses on a single grain from sample 41A and the identical results from two analyses on the same grain from sample 263A.

Always consult and cite the final, published document. See http://www.minsocam.org or GeoscienceWorld

FIGURE 8. Cartoon illustrating the difference between rim domains in the chlorite-kyanite zones and sillimanite-sillimanite−K-feldspar zones. Zircon interiors are of pre-Grampian age. Thin, discontinuous overgrowths may be of Grampian or post-Grampian age.

Always consult and cite the final, published document. See http://www.minsocam.org or GeoscienceWorld

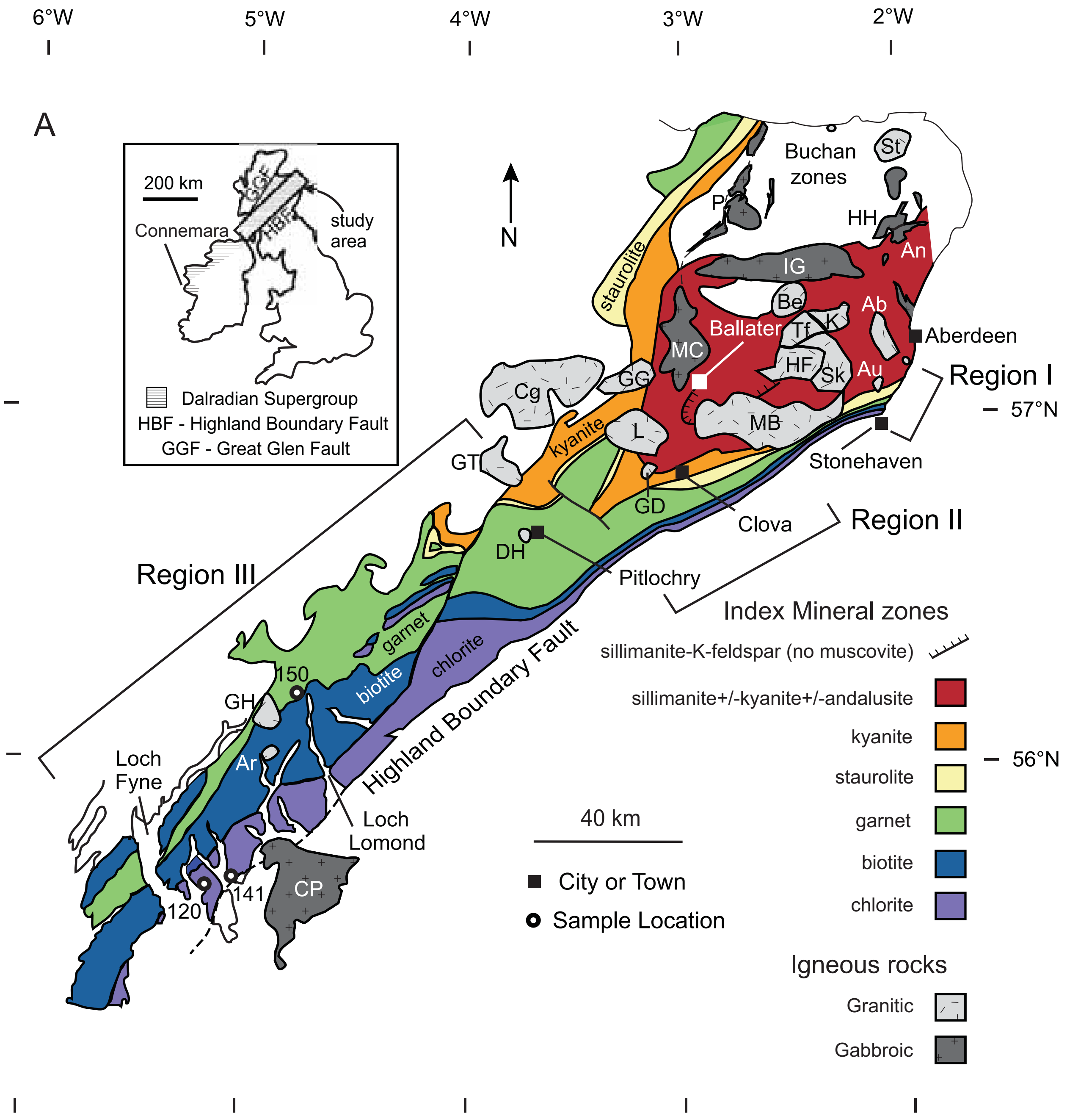
6°W
5°W
4°W
3°W
2°W
A
200 km
GGF
HBF
study area
Connemara
Dalradian Supergroup
HBF - Highland Boundary Fault
GGF - Great Glen Fault
N
Buchan zones
St
P
HH
An
IG
Be
Ab
Ballater
Tf
K
Aberdeen
MC
HF
Sk
Au
Region I
57°N
Cg
GG
staurolite
kyanite
L
MB
Stonehaven
GT
GD
Clova
Region II
DH
Pitlochry
Region III
garnet
biotite
chlorite
Highland Boundary Fault
150
GH
Loch Fyne
Ar
Loch Lomond
CP
141
120
56°N
Index Mineral zones
sillimanite-K-feldspar (no muscovite)
sillimanite+/-kyanite+/-andalusite
kyanite
staurolite
garnet
biotite
chlorite
40 km
City or Town
Sample Location
Igneous rocks
Granitic
Gabbroic

Fig. 1 A

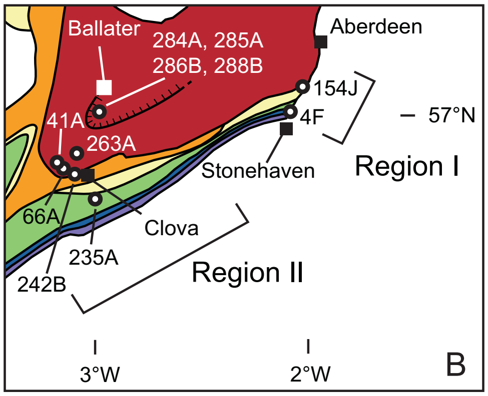
Ballater
284A, 285A
286B, 288B
Aberdeen
154J
4F
57°N
41A
263A
Stonehaven
Region I
66A
Clova
235A
242B
Region II
3°W
2°W
B

Fig. 1B

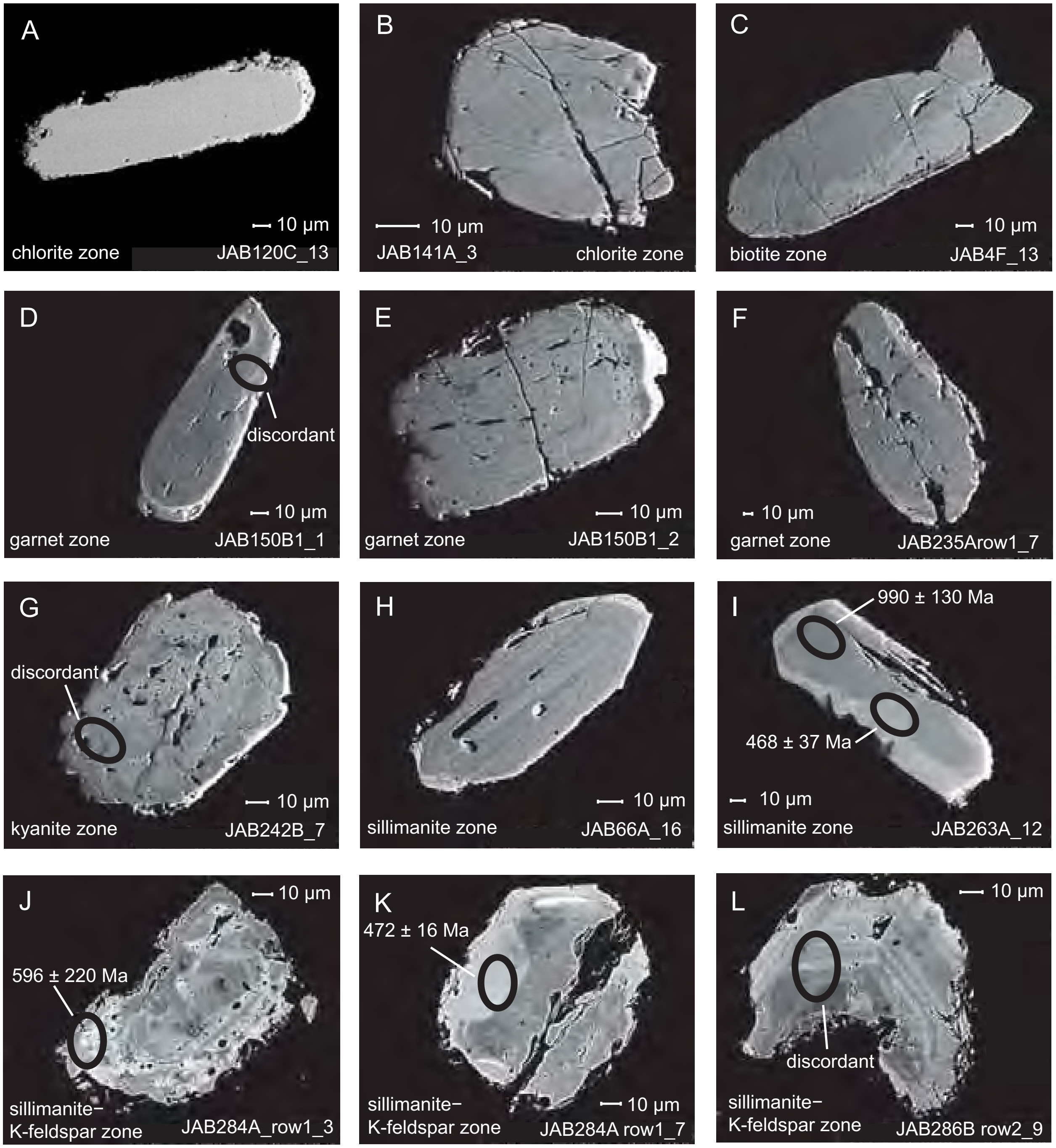
A
10 μm
chlorite zone
JAB120C_13
B
10 μm
JAB141A_3
chlorite zone
C
10 μm
biotite zone
JAB4F_13
D
discordant
10 μm
garnet zone
JAB150B1_1
E
10 μm
garnet zone
JAB150B1_2
F
10 μm
garnet zone
JAB235Arow1_7
G
discordant
10 μm
kyanite zone
JAB242B_7
H
10 μm
sillimanite zone
JAB66A_16
I
990 ± 130 Ma
468 ± 37 Ma
10 μm
sillimanite zone
JAB263A_12
J
10 μm
596 ± 220 Ma
sillimanite–
K-feldspar zone
JAB284A_row1_3
K
472 ± 16 Ma
sillimanite–
K-feldspar zone
10 μm
JAB284A row1_7
L
10 μm
discordant
sillimanite–
K-feldspar zone
JAB286B row2_9

Fig. 2

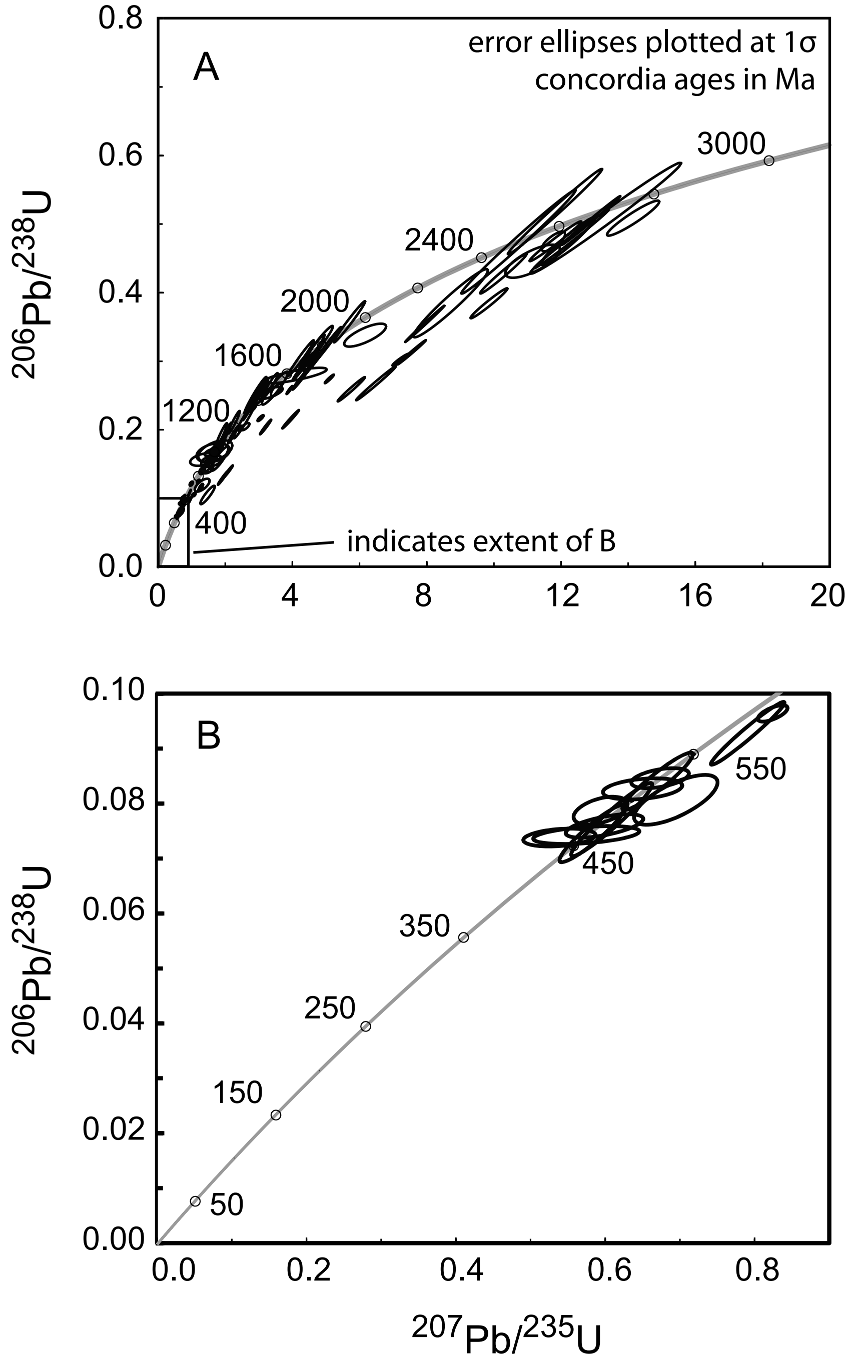
A
error ellipses plotted at 1σ
concordia ages in Ma
3000
2400
2000
1600
1200
400
indicates extent of B
0.8
0.6
0.4
0.2
0.0
0
4
8
12
16
20
206Pb/238U
B
550
450
350
250
150
50
0.10
0.08
0.06
0.04
0.02
0.00
0.0
0.2
0.4
0.6
0.8
206Pb/238U
207Pb/235U

Fig. 3

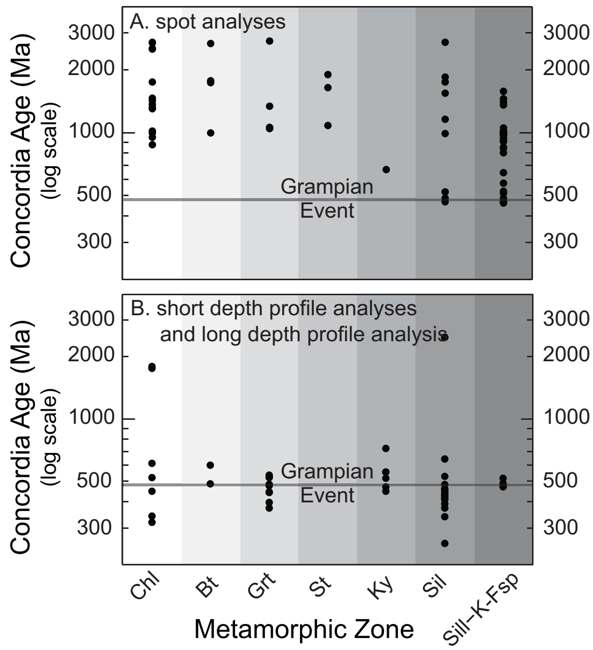
A. spot analyses
B. short depth profile analyses and long depth profile analysis
Concordia Age (Ma) (log scale)
3000
2000
1000
500
300
Grampian Event
Chl
Bt
Grt
St
Ky
Sil
Sill–K-Fsp
Metamorphic Zone

Fig. 4

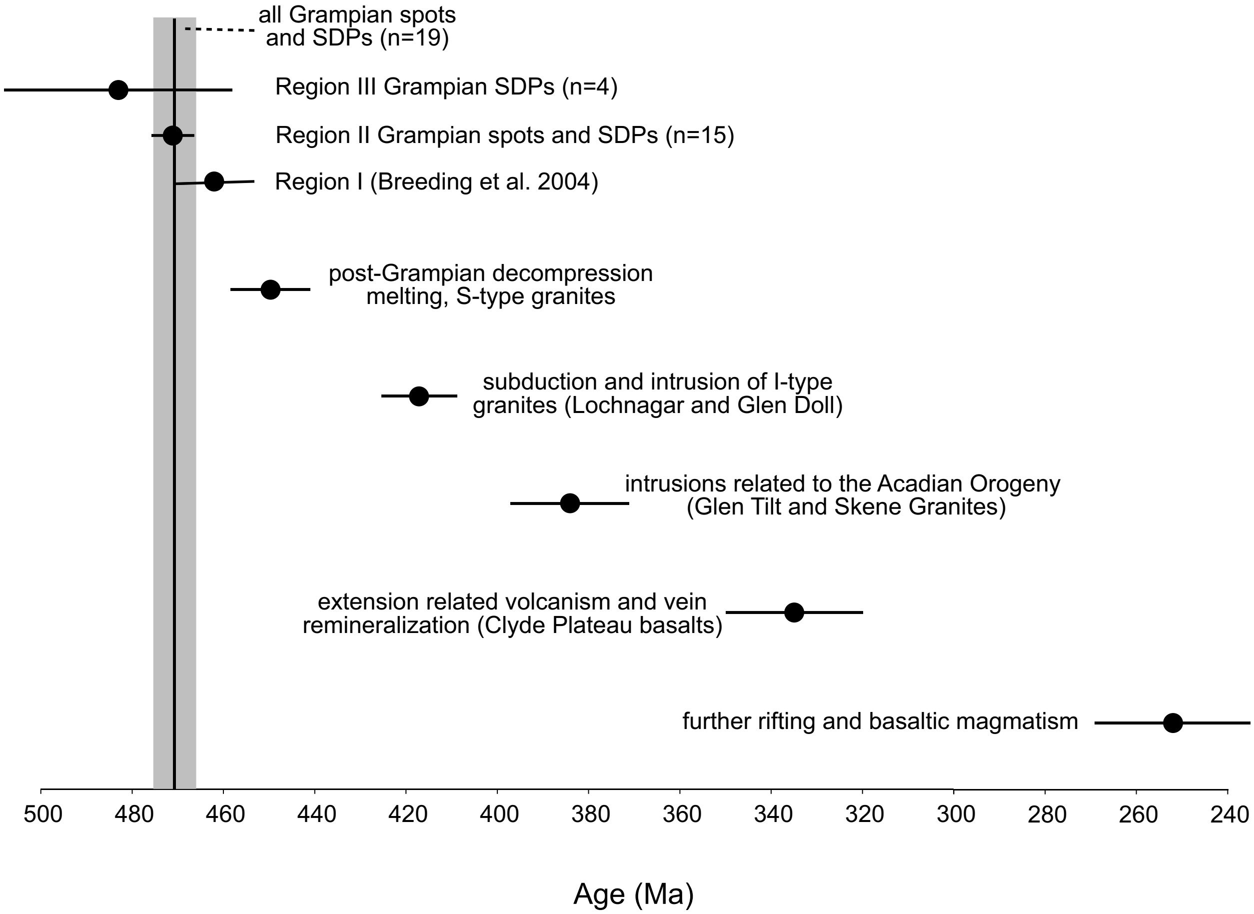

Fig. 5

Always consult and cite the final, published document. See http://www.minsocam.org or GeoscienceWorld

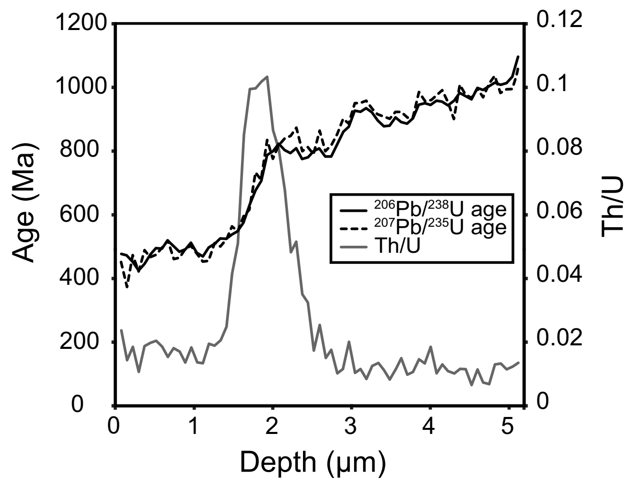
1200
1000
800
600
400
200
0
Age (Ma)
0.12
0.1
0.08
0.06
0.04
0.02
0
Th/U
0 1 2 3 4 5
Depth (μm)
206Pb/238U age
207Pb/235U age
Th/U

Fig. 6

This is a preprint, the final version is subject to change, of the American Mineralogist (MSA)
Cite as Authors (Year) Title. American Mineralogist, in press.
(DOI will not work until issue is live.) DOI: http://dx.doi.org/10.2138/am.2013.4240

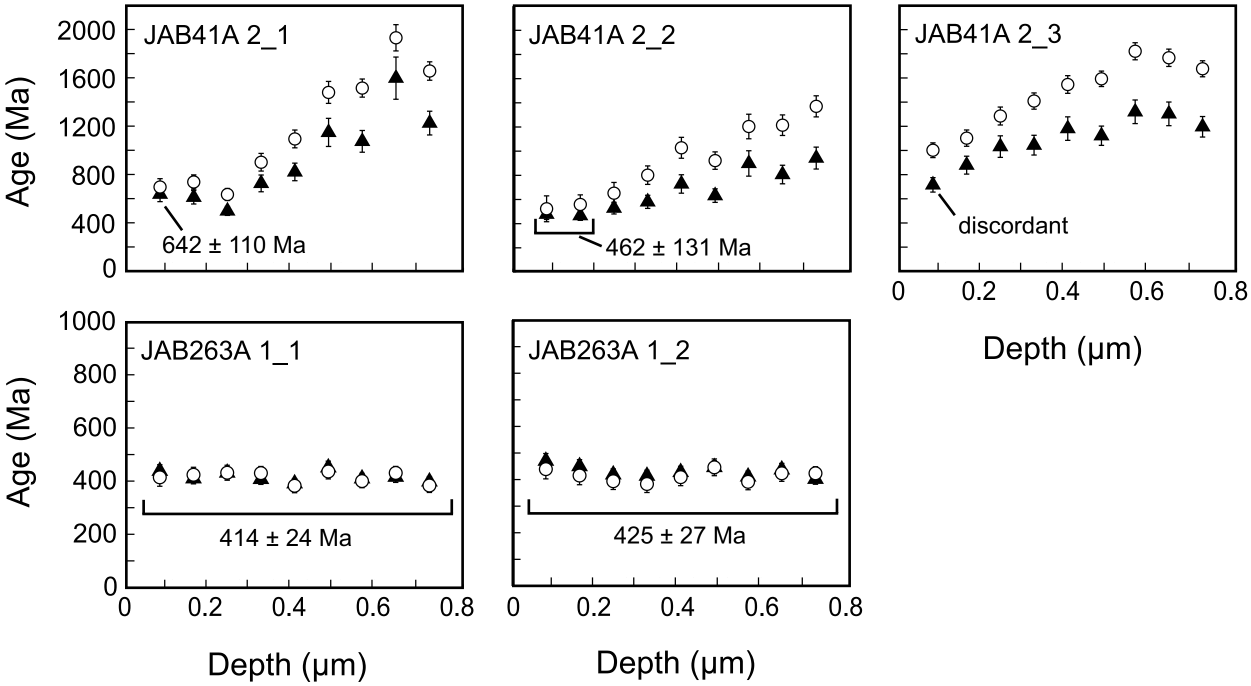

Fig. 7

Always consult and cite the final, published document. See http://www.minsocam.org or GeoscienceWorld

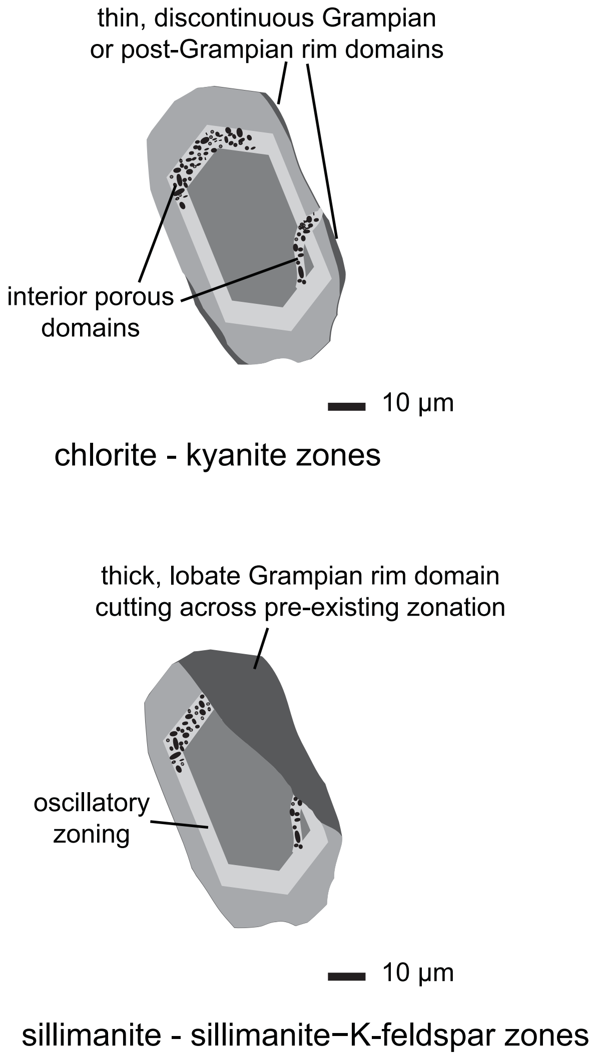
thin, discontinuous Grampian
or post-Grampian rim domains
interior porous
domains
10 μm
chlorite - kyanite zones
thick, lobate Grampian rim domain
cutting across pre-existing zonation
oscillatory
zoning
10 μm
sillimanite - sillimanite−K-feldspar zones

Fig. 8

TABLE 1. Ages of relevant igneous rocks within the study area

Age (Ma)	±	Name/Location	Fig. 2 Abbr.	Rock Type	Technique	Reference
491	15	Dunfallandy Hill	DH	granite	Rb-Sr whole rock	Pankhurst and Pidgeon, 1976
487	23	Haddo House	HH	gabbro	Rb-Sr whole rock on metamorphic aureole	Pankhurst, 1970
482	12	Arnage	An	granites /gneisses	Rb-Sr whole rock	Pankhurst, 1970
475	12	Auchlee	Au	granite	U-Pb zircon	Oliver et al., 2008
474	2	Portsoy	P	gabbro	U-Pb zircon	Martin and Condon in Oliver et al., 2008
472	*n.d*	Morven Cabrach	MC	gabbro	U-Pb zircon	Rogers et al., 1994
471	12	Tillyfourie	Tf	granite	U-Pb zircon	Oliver et al., 2008
470	1	Aberdeen	Ab	granite	U-Pb monazite	Kneller and Aftalion, 1987
470	9	Insch	IG	gabbro	U-Pb zircon	Dempster et al., 2002
468	*n.d*	Insch	IG	gabbro	U-Pb zircon	Rogers et al., 1994
467	6	Strichen	St	granite	U-Pb zircon	Oliver et al., 2000
457	1	Kennethmont	K	granite	U-Pb zircon	Oliver et al., 2000
429	2	Garabal Hill	GH	appinite	U-Pb zircon	Rogers and Dunning, 1992
426	3	Arrocher	Ar	appinite	U-Pb titanite	Rogers and Dunning, 1991
420	2	Lochnagar	L	granite	U-Pb zircon	Abbleby (pers.comm.) from Oliver et al., 2008
419	5	Glen Doll	GD	diorite	U-Pb zircon	Oliver et al., 2008
415	1	Glen Gairn	GG	granite	U-Pb monazite	Parry (pers. comm.) from Oliver et al., 2008
408	5	Bennachie	Be	granite	U-Pb zircon	Oliver et al., 2008
406	5	Mount Battock	MB	granite	U-Pb zircon	Oliver et al., 2008
404	18	Cairngorn	Cg	granite	U-Pb zircon	Oliver et al., 2008
403	8	Hill of Fare	HF	granite	U-Pb zircon	Oliver et al., 2008
396	6	Skene	Sk	granite	U-Pb zircon	Oliver er al., 2008
390	5	Glen Tilt	GT	granite	U-Pb zircon	Oliver et al., 2008
335	1	Clyde Plateau	CP	trachyandesite lava	U-Pb zircon	Monaghan and Parrish, 2006

Note : Abbreviations indicate locations on Fig. 2.
n.d : indicates that no uncertainty data was provided

Always consult and cite the final, published document. See http://www.minsocam.org or GeoscienceWorld